

Self-Sustaining Oscillations in Complex Networks of Excitable Elements

Patrick McGraw and Michael Menzinger

Department of Chemistry, University of Toronto, Toronto, Ontario, Canada M5S 3H6.

(Dated: September 14, 2021)

Abstract

Random networks of symmetrically coupled, excitable elements can self-organize into coherently oscillating states if the networks contain loops (indeed loops are abundant in random networks) and if the initial conditions are sufficiently random. In the oscillating state, signals propagate in a single direction and one or a few network loops are selected as driving loops in which the excitation circulates periodically. We analyze the mechanism, describe the oscillating states, identify the pacemaker loops and explain key features of their distribution. This mechanism may play a role in epileptic seizures.

PACS numbers: 89.75.Hc, 05.65.+b, 87.19.lj, 87.19.xm

The coherent oscillation (CO) of a collection of units that are non-oscillatory on their own is relevant to biological and physical sciences: CO has been identified and analyzed in populations of excitable biological cells (yeast[1], β pancreatic cells[2], Dictyostelium discoideum[3] and cultured heart cells[4]) and of excitable catalytic particles[5][6][7]. In contrast with well-studied synchronization phenomena of self-oscillating units[8], in these cases the ability to oscillate derives from the interactions of the elements. CO can occur also on complex networks if the nodes are excitable [9][10] or even monostable[9], provided that the network contains *loops*, and that the directional symmetry of couplings is somehow broken to allow a signal to propagate in a single direction around a loop[10]. Networks of these types include some neural [11][12] and genetic regulatory networks.[9] Some studies of excitable networks have been inspired by target and spiral waves in continuous media. [13][7][10]

In complex networks, loops are both generic and abundant.[15][14] While short loops of length $L \ll N$ (where N is the network size) are rare in large random networks, ones with $L \gtrsim \ln N$ occur generically in numbers growing exponentially with N . Their number also grows roughly exponentially with L up to a maximum at a length $L_m \sim N$. [15][14]

In this letter we show that random excitable networks readily self-organize into a CO state following a transient phase during which one or a few loops are dynamically selected as driving (or pacemaker) loops. We describe the mechanism of signal propagation and gain an understanding of the resulting distributions of the oscillating states and associated driving loops.

We consider networks of diffusively coupled, excitable elements with dynamics described by the Bär model [16]

$$\frac{du_i}{dt} = \frac{1}{\varepsilon} u_i (1 - u_i) \left(u_i - \frac{v_i + b}{a} \right) + D \sum_{j=1}^N A_{ij} (u_j - u_i), \quad (1)$$

$$\frac{dv_i}{dt} = f(u_i) - v_i,$$

where

$$f(u_i) = \begin{cases} 0 & u_i \leq 1/3 \\ 1 - 6.75u_i(u_i - 1)^2 & 1/3 < u_i < 1 \\ 1 & u_i \geq 1 \end{cases},$$

N is the number of nodes, u_i and v_i are dynamical variables, D is the coupling strength, and A_{ij} is the adjacency matrix. a , b , and ε are parameters, for which we adopt the values $a = 0.84$, $b = 0.07$, and $\varepsilon = 0.04$. In the absence of coupling, the individual nodes display excitable dynamics, with a stable equilibrium at $(u, v) = (0, 0)$ and an excitation threshold $u_{th} \approx 0.1$. The dynamical equations were integrated numerically using a fourth-order Runge-Kutta algorithm with time step $\Delta t = 0.1$.

For the topology, we chose the undirected random regular network of degree 3 (RRN3), where nodes are randomly and symmetrically connected with the constraint that all have the same degree $k = 3$. The network size was $N = 200$. Other topologies and other values and distributions of k will be considered elsewhere.

To excite the network, we used random initial conditions in which each node was either displaced from equilibrium with probability p , or left at $(0, 0)$ with probability $1 - p$. For the nodes that were displaced, initial values of u and v were distributed randomly and independently within the intervals $0.2 \leq u \leq 0.9$, $0 \leq v \leq 1$, thus placing them above the excitation threshold but with some phase randomness. (This randomness proves important, as discussed below.) After determining that the results were largely insensitive to the value of p , we subsequently took $p = 0.5$.

Integrating the equations of motion (1), we found two possible outcomes: either the system relaxed rapidly to the quiescent state with all nodes at the fixed point or it reached a coherently oscillating state (COS) like the one illustrated in fig.2. In the COS, all nodes fire at the same frequency, with a fixed phase relationship among them. To examine the phase relations, we define a firing time t_i of the i th node as the time (interpolated linearly between discrete time steps) at which u_i crosses from below 0.5 to above 0.5. The interval between successive firing times (interspike interval or ISI) converges to a stable common

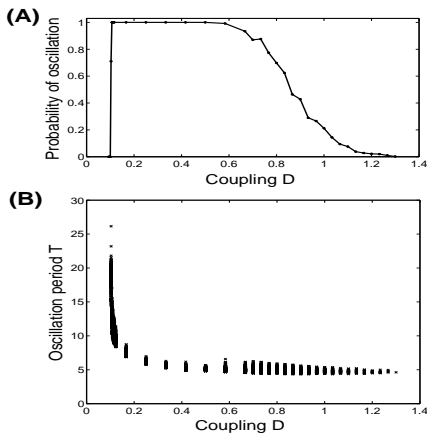


FIG. 1: (A) Probability that a random initial condition with excitation probability $p = 0.5$ relaxes to an oscillatory state, averaged over 1000 initial conditions of 5 network realizations. (B) Scatter plot of oscillation periods T . Periods are longer and more variable at weaker coupling.

value for all nodes, which is the oscillation period T . We considered the system to have converged to a COS if the standard deviation of the ISI's over the network remained below 10^{-4} for more than 100 time units. As shown in fig.1, COS are highly probable for a range of coupling strengths $0.1 \lesssim D \lesssim 0.6$, while the periods decrease with increasing D .

The local structure of the oscillatory state is illustrated by fig.2B, which shows the firing pattern of an arbitrarily chosen node and its three neighbors. As each node fires once per oscillation, one can define a time delay Δ_{ij} (with $-T/2 \leq \Delta_{ij} < T/2$) for each link in the network as the difference of firing times $t_i - t_j$ between the nodes at its two ends, modulo the oscillation period T . With the establishment of stable signed delays, the initially undirected network self-organizes into a directed one in which the signal propagates in only one direction along each link. Since each node i must be excited by one of its neighbors, it must have at least one incoming link (positive Δ_{ij}) but can have between 0 and 2 outgoing links (negative Δ_{ij}). The node illustrated in fig.2B is a “diverging” node with one incoming and two outgoing links. Since the total numbers of incoming and outgoing links in the network must balance, all nodes cannot be converging. This implies that CO can only occur if a single firing neighbor suffices to excite a node. In this case, the firing of a node at the “upstream” end of a link guarantees that the one at the “downstream” end will fire within a certain time period, provided the downstream node is not refractory when it receives the input. If the downstream node receives a second input before it fires, it will be pulled over the threshold more quickly and fire sooner. Converging inputs thus account for most of the variation in transmission delays.

Liao et al. [9] suggested a way of identifying the main transmission pathways by selecting the so-called domi-

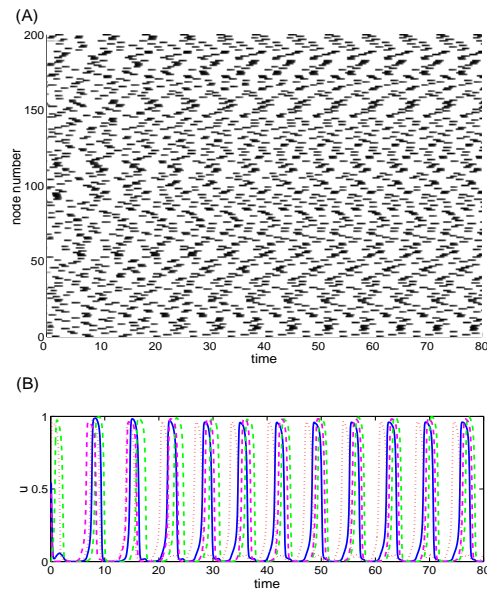


FIG. 2: (color online): Example of a periodic network oscillation for coupling strength $D = 0.2$. (A) Raster plot of all nodes’ activity. Gray level is proportional to $u_i(t)$. The network quickly settles to a steady oscillation in which all nodes fire with the same period in a fixed phase relationship to each other. (B) $u(t)$ for an arbitrarily chosen node (solid line) and its three neighbors (incoming: dotted and outgoing: dashed lines).

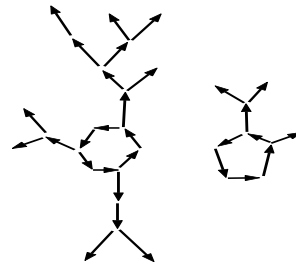


FIG. 3: Branched circle structure of the pruned network. Following dominant phase-advanced driving links backwards from any node inevitably leads to a unidirectional loop from which the signal radiates along branches.

nant phase-advanced driving (DPAD) links, which then leads to identifying the pacemaker or driving loops (DL). The DPAD for each node is the incoming link with the largest delay. A justification for considering the earliest input to be the most important is that one input is sufficient to guarantee the node’s firing, and additional inputs can only affect the timing. Pruning the network to include only DPAD links simplifies it to a so-called branched circle structure[9] consisting of trees attached to unidirectional DLs as illustrated in fig. 3.

To study the statistics of the COS’s and their basins of attraction we integrated eqs. (1) with $D = 0.11$ for 1000 different initial conditions (200 each for five different

RRN3 realizations). All but one of these initial conditions converged to a COS. We then measured the firing delays and pruned the network as described above to identify the driving loops. We found up to four distinct DLs in each COS, all mutually entrained to oscillate with the same period. 50.9 percent of the COS had only one DL, with the probability of more loops decreasing monotonically with number. In each case, we measured the length L of the shortest DL. The distribution of these lengths is shown in figure 4A. As figure 4B shows, the oscillation period T is correlated with L , but the data fall into clusters separated according to the number of pulses circulating simultaneously around the loop, which we call the multiplicity M . M can be measured by adding up the transmission delays along the driving loop to get the time for a single pulse to make one circuit, and dividing this by the oscillation period. Fig.4C shows that the data collapse into a single band when one plots T vs. L/M . One can interpret the slope of this band as the typical delay added by a link. A notable feature of this plot is that the best fit line does not pass through the origin as one would expect if waves of excitation travelled at a constant velocity independent of the loop length. This feature becomes even more noticeable when we examine data at stronger coupling (where transmission delays are shorter). Data for $D = 0.6$ look qualitatively similar to those shown in figure 4, except that the minimum value of L is 6 rather than 4, and the slope of the plot of T vs. L/M is considerably smaller, as expected, while the intercept is only slightly smaller. The resulting overall spread of oscillation periods is correspondingly less. At larger coupling strength, the transmission delay is smaller and evidently plays less of a role in setting the period.

Several features of our results merit discussion. First, we note the ease with which the network is induced to oscillate: the probability of obtaining oscillations from random initial conditions is nearly 1 within a range of coupling strengths, and there is a large number of distinct oscillatory attractors as attested by the scatter of periods and the variety of DLs. Second, no external driving is needed to sustain CO activity, unlike the case considered by [10]. Unlike cases where oscillation resulted from adding directed shortcuts to a spatial network[7][13][17], here the connections are symmetric. This symmetry is only broken dynamically, producing different directed networks and selecting different driving loops depending on the initial conditions.

A non-trivial distribution of the initial conditions in phase space is evidently crucial: initial conditions where one or more nodes were excited synchronously (displaced to the same point above the excitation threshold) failed to produce oscillations. A single excited node on a loop produces two wavefronts of excitation propagating in opposite directions, which will annihilate elsewhere on the loop. If an excited node adjoins a refractory one, however, the signal is blocked from moving in one direction and a unidirectional loop can be established.[10] Evidently the random initial distribution we have used is

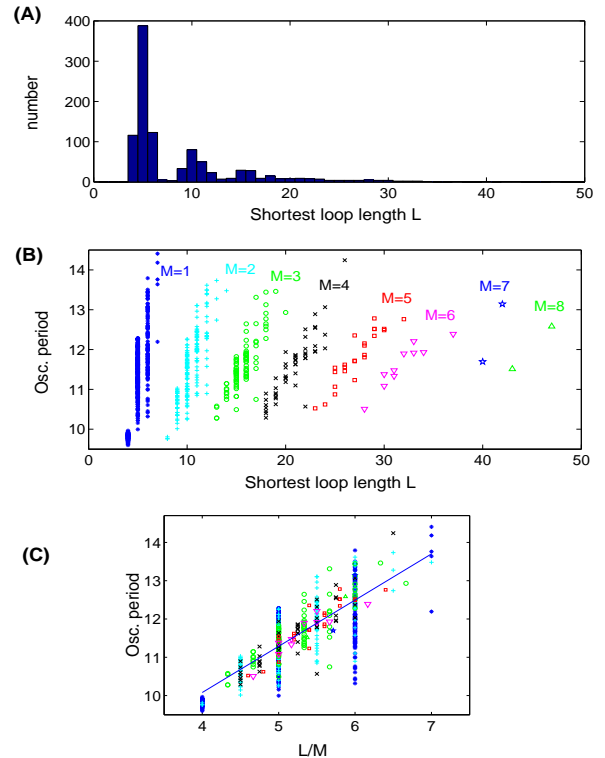


FIG. 4: (color online): Pacemaker loops and oscillation periods for $D = 0.11$, for 1000 different initial conditions of 5 network realizations. (Features are qualitatively similar for COS at $D = 0.6$) (A) Histogram of lengths of shortest driving loops. (The shape is qualitatively similar if all loops are included.) A semilogarithmic plot of the cumulative distribution (not shown here) reveals an exponentially decaying trend. (B) Oscillation period T vs. shortest loop length. Different symbols show loops of different multiplicities M . Note that the clusters at different M values correspond to the local peaks in panel (A). (C) The data from (B) collapse into a single band when one plots T vs. L/M . The best fit line shown here is $T = 1.21(L/M) + 5.26$. For $D = 0.6$, the corresponding best fit is $T = 0.25(L/M) + 2.85$.

sufficient to allow this.

As shown in figure 1, the probability of obtaining oscillations from a random initial condition jumps rapidly from 0 to 1 at a lower threshold coupling strength $D_l = 0.1$, and falls off more gradually for $D \gtrsim 0.6$. The lower threshold represents the minimum coupling necessary for a node to be excited by the firing of a single neighbor. The slower decay of the oscillation probability at $D \gtrsim 0.6$ can be explained by the shortening of transmission delay compared to the refractory period. In the cases where oscillation fails, it does so due to an avalanche that spreads so rapidly through the network that almost all nodes are firing at once. The activity burns out quickly when there are no nodes remaining that are not already firing or refractory.

The oscillation period is bounded from below by the refractory period. This also implies a lower bound on

the length of a DL depending on the maximum delay per link: oscillation cannot be sustained if a pulse travelling along a loop returns to a given node while that node is still refractory. The observed lower bound on the loop size, $L_{\min} = 4$ in the case $D = 0.11$, in fact increases to 6 when D is increased to 0.6, because increasing D decreases the transmission delay. More generally, the above argument explains the observed lower bound on the ratio L/M , which represents the spacing between pulses on a DL. L/M , on the other hand, is also apparently bounded from above, as evident from figure 4C. A possible explanation for this lies in the transient process by which a particular loop becomes established as the primary DL. During this transient phase, many pulses are propagating in an unsynchronized manner through the network, and a number of potential pacemakers are competing. A large gap between circulating pulses is therefore likely to be filled in. This is analogous to oscillations in excitable spatial media, where pacemakers with the shortest periods dominate.[13]

The distribution of driving loops (figure 4A) decays with L , despite the fact that the number of loops present in the network *grows* exponentially with L . There is evidently a strong bias in favor of shorter loops. This bias appears to be a statistical effect inherent in the topology of the directed branched circle network rather than strictly a dynamical effect. To check this hypothesis, we compared our results with a “null model” that generates branched circle networks independently of the oscillatory dynamics. For the null model, we generate directed networks as follows. First, assign a random direction to each link in an RRN3, and then, where necessary, reverse directions of some links to ensure that every node has at least one incoming link. For each node, we then randomly choose one among its incoming links to be the dominant one, and prune the others if the node is converging. The result is a network satisfying the same topological constraints as the pruned network of DPAD connections, but generated by a random process rather than a dynamical one. The distribution of the shortest

loop length L for an ensemble of such networks decays exponentially as it does in the DPAD network. Simply by assigning directions and then pruning, one samples the loops of the original undirected network unevenly. Longer loops have more chances either to fail to be unidirectional when directions are assigned, or to be eliminated by pruning.

The driving loops uncovered by the DPAD reduction explain part but not all of the variation in oscillation periods (see fig.4). Secondary (non-dominant) connections alter the firing times, and are also responsible for the entrainment of multiple DL when the latter occur. If the connections that we prune for the sake of analysis were truly removed from the network, it would be impossible for the resulting disconnected components to synchronize. It is also worth emphasizing that when $M > 1$, the multiple pulses are precisely evenly spaced as they travel around the loop, so that the interval between firings is constant for a given node. This is another form of entrainment that we would not expect if the pruned connections were truly absent.

The dynamical organization of an undirected network giving rise to a directed one with considerably different loop statistics provides an intriguing case study of the distinction between “functional” networks defined by dynamical interactions and the underlying structural networks of hard-wired connections. Functional networks of observed correlations of activity among brain regions have been studied as a tool to infer the underlying architecture[18], but the phenomenon discussed here illustrates that functional and structural networks may have markedly different properties.

Unlike the cases of interacting excitable cells where the oscillation is treated as a collective phenomenon[1]-[6], in the case of a fixed network specific signalling pathways can be more readily identified. The networks studied here share some essential features with brains, and it is plausible that the mechanism described here plays a role in epileptic seizures.[19]

-
- [1] S. de Monte, F. d’Ovidio, S. Dano, and P.G. Sorensen. Proc. Natl. Acad. Sci. USA **104**, 18377 (2007).
[2] J.H.E. Cartwright. Phys. Rev. E **63**, 1149 (2000).
[3] V. Nanjundiah. Biophys. Chem. **72**, 1 (1998).
[4] G. Bub, A. Shrier, and L. Glass. Phys. Rev. Lett. **94**, 028105 (2005).
[5] M.R. Tinsley, A.F. Taylor, Z. Huang, F.Wang, K. Showalter. Physica D **239**, 785 (2010).
[6] A.F. Taylor, M.R. Tinsley, F. Wang, Z. Huang, K. Showalter, Science **323**, 614 (2009).
[7] A.J. Steele, M. Tinsley and K. Showalter. Chaos **16**, 015110 (2006).
[8] S. H. Strogatz, *Sync: The Emerging Science of Spontaneous Order* (Hyperion, New York, 2003); A. Pikovsky, M. Rosenblum and J. Kurths, *Synchronization: A Universal Concept in Nonlinear Sciences* (Cambridge UP, Cambridge, 2001).
[9] X. Liao et al. e-print arXiv:0906.2356 [nlin.AO] (2009).
[10] T.J. Lewis and J. Rinzel. Network: Comput. Neural Syst. **11**, 299 (2000).
[11] E. Marder and D. Bucher. Curr. Biol. **11**, R986 (2001).
[12] A.I. Selverston and M. Moulins. Ann. Rev. Physiol. **47**, 29 (1985).
[13] S. Sinha, J. Saramäki, and K. Kaski. Phys. Rev. E **76**, 015101(R) (2007).
[14] E. Marinari, R. Monasson and G. Semerjian. Europhys. Lett. **73**, 8 (2006); G. Bianconi and M. Marsili. J. Stat. Mech. **2005**, 14 (2005); G. Bianconi and A. Capocci, Phys. Rev. Lett. **90**, 078701 (2003).
[15] E. Marinari and R. Monasson. J. Stat. Mech. **2004**, P09004 (2004).
[16] M. Bär and M. Eiswirth. Phys. Rev. E **48**, R1635 (1993).

- [17] A. Roxin, H. Riecke, and S.A. Solla. Phys. Rev. Lett. **92**, 198101 (2004).
- [18] V.M. Eguiluz, D.R. Chialvo, G.A. Cecchi, M. Baliki and A.V. Apkarian. Phys. Rev. Lett. **94**, 018102 (2005).
- [19] T.I. Netoff, R. Clewley, S. Arno, T. Keck, and J.A. White. J. Neuroscience, **24**, 8075 (2004); M. Steriade. *Neuronal Substrates of Sleep and Epilepsy*. (Cambridge UP, New York, 2003); I. Soltesz and K. Staley, eds. *Computational Neuroscience in Epilepsy* (Elsevier, 2008)